

# Charts for Determination of Crystal Orientation by Surface Traces in Cubic Crystals

著者	TAKEUCHI Sakae, HONMA Toshio, IKEDA Susumu
journal or publication title	Science reports of the Research Institutes, Tohoku University. Ser. A, Physics, chemistry and metallurgy
volume	11
page range	81-93
year	1959
URL	<a href="http://hdl.handle.net/10097/26905">http://hdl.handle.net/10097/26905</a>

# Charts for Determination of Crystal Orientation by Surface Traces in Cubic Crystals\*

Sakae TAKEUCHI, Toshio HONMA and Susumu IKEDA

*The Research Institute for Iron, Steel and Other Metals*

(Received December 23, 1958)

## Synopsis

A useful method for the determination of the orientations of crystal grains in polycrystalline specimens having cubic lattice structure was found from the observation of angles between the surface traces such as slip lines, annealing twins or etch-pits which are developed in  $\{111\}$  or  $\{100\}$  planes. From the computation of relations between the angular co-ordinates ( $\xi, \eta$ ) of the crystal orientation and the intertrace angles ( $\alpha, \beta$ , etc.) in various directions of  $\{111\}$  or  $\{100\}$  traces, isogonic lines of the intertrace angles were plotted at the interval of two degrees. The case of  $\{111\}$  traces only in three directions was also discussed, and the relations between the angles of the three traces and the number of possible orientations corresponding to the same traces were explained. When the angle between the  $\{100\}$  traces was large, considerable errors were unavoidable in determining the orientations, but an accurate determination was possible if  $\{100\}$  and  $\{111\}$  traces were used in combination. The relations for such a combination were also calculated and plotted in the form of chart. By using these charts, the crystallographic orientations of crystal grains could be determined very rapidly and accurately.

## I. Introduction

The orientation of a single crystal or a large crystal grain can be determined accurately by X-ray diffraction or by light-figure method<sup>(1)</sup>, but these methods may be inapplicable to the case of polycrystals because of small grain size.

For the determination of the orientation of a microscopical grain, the methods of utilizing the form of chemical, thermal or electrolytic etch-pits<sup>(2)</sup>, the dendrite<sup>(3)</sup>, the slip bands or twins have been proposed, and various procedures have been devised for the determination of the orientation from the surface traces of a specimen. These procedures, however, are comparatively complicated and are powerless to avoid errors of a considerable extent. In these methods, the orientation is determined from the measurements of the angles between the various directions of the surface traces of known crystallographic planes. Therefore, the orientation would be determined by measuring only the angles between the various surface traces on the microphotograph without further procedures, if a chart

\* The 928th report of the Research Institute for Iron, Steel and Other Metals

- (1) M. Yamamoto, Sci. Rep. Tôhoku Univ., **31** (1943), 121.  
M. Yamamoto and J. Watanabé, Sci. Rep. RITU, **A7** (1955), 173; **A9** (1957), 410.
- (2) G. E. G. Tucker and P. C. Murphy, J. Inst. Metals, **81** (1953), 235.  
A. Nakamura, J. Japan Inst. Metals, **18** (1954), 145.  
C. S. Barrett, *Structure of Metals*, McGraw-Hill (1943), 173.
- (3) L. Northcott and D.E. Thomas, J. Inst. Metals, **65** (1939), 205.

embodying the results of calculations for determining the relations between the orientation and the said angles was obtained. For this purpose, the charts were prepared for the cases of traces developed in the  $\{111\}$  and the  $\{100\}$  planes, which are frequently observed in cubic crystals. In chapter II in this report, the chart will be described for the cases where the four traces of the  $\{111\}$  planes, such as slip bands and annealing twins in face-centred cubic crystals, are completely observable. In chapter III, the chart will be described for the cases of  $\{100\}$  traces, such as etch-pits in cubic crystals, and the charts for the cases of the combination of  $\{100\}$  and  $\{111\}$  traces.

## II. The chart for $\{111\}$ traces

### 1. Preparation of the charts

The orientation of a crystal can be indicated by the stereographic projection as shown in Fig. 1, in which the great circle MN represents the surface plane of

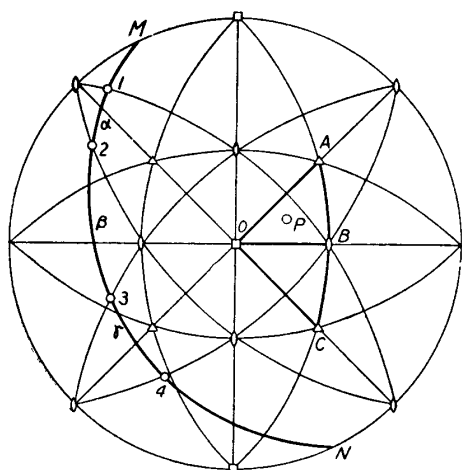


Fig. 1. Stereographic projection showing the poles of the normal of crystal surface and the  $\{111\}$  traces.

a crystal oriented at the point P. If the four  $\{111\}$  planes are taken to intersect with the surface MN at 1, 2, 3 and 4 respectively, these would represent the traces formed on the surface. Let  $\alpha$ ,  $\beta$ ,  $\gamma$ , and  $\delta$  stand for the angles between 1 and 2, 2 and 3, 3 and 4, and 4 and -1, respectively, and  $\xi$  and  $\eta$  for the longitude and the latitude defining the point P, then the following equations will be given, except in the case where  $\xi = 45^\circ$  and  $\eta = \pm 35^\circ 16'$  (the point  $\langle 111 \rangle$ ):

$$\cos\alpha = 2(1 - \tan\xi \sec\xi \tan\eta) / \Delta_1 \Delta_2$$

$$\cos\beta = 2(\tan\xi - \sec^2\xi \tan^2\eta) / \Delta_2 \Delta_3$$

$$\cos\gamma = 2(1 + \tan\xi \sec\xi \tan\eta) / \Delta_3 \Delta_4$$

$$\delta = 180^\circ - (\alpha + \beta + \gamma)$$

where

$$\Delta_1 = \sqrt{(\tan\xi - \sec\xi \tan\eta)^2 + (1 + \sec\xi \tan\eta)^2 + (1 + \tan\xi)^2}$$

$$\Delta_2 = \sqrt{(\tan\xi - \sec\xi \tan\eta)^2 + (1 - \sec\xi \tan\eta)^2 + (1 - \tan\xi)^2}$$

$$\Delta_3 = \sqrt{(\tan\xi + \sec\xi \tan\eta)^2 + (1 + \sec\xi \tan\eta)^2 + (1 - \tan\xi)^2}$$

$$\Delta_4 = \sqrt{(\tan\xi + \sec\xi \tan\eta)^2 + (1 - \sec\xi \tan\eta)^2 + (1 + \tan\xi)^2}$$

Now, compute  $\alpha$ ,  $\beta$ ,  $\gamma$  and  $\delta$  in respect of  $\xi$  and  $\eta$  for many points in the OABC by using the above equations, and draw the isogonic lines of the angles of  $\alpha$ ,  $\beta$ ,  $\gamma$  and  $\delta$  with  $\xi$  on the abscissa and  $\eta$  on the ordinate. The chart thus obtained shows that in cases of all the points within OABC (except when they are on OA or OC),  $\delta$  has the largest value, and that isogonic lines of  $\alpha$  intersect

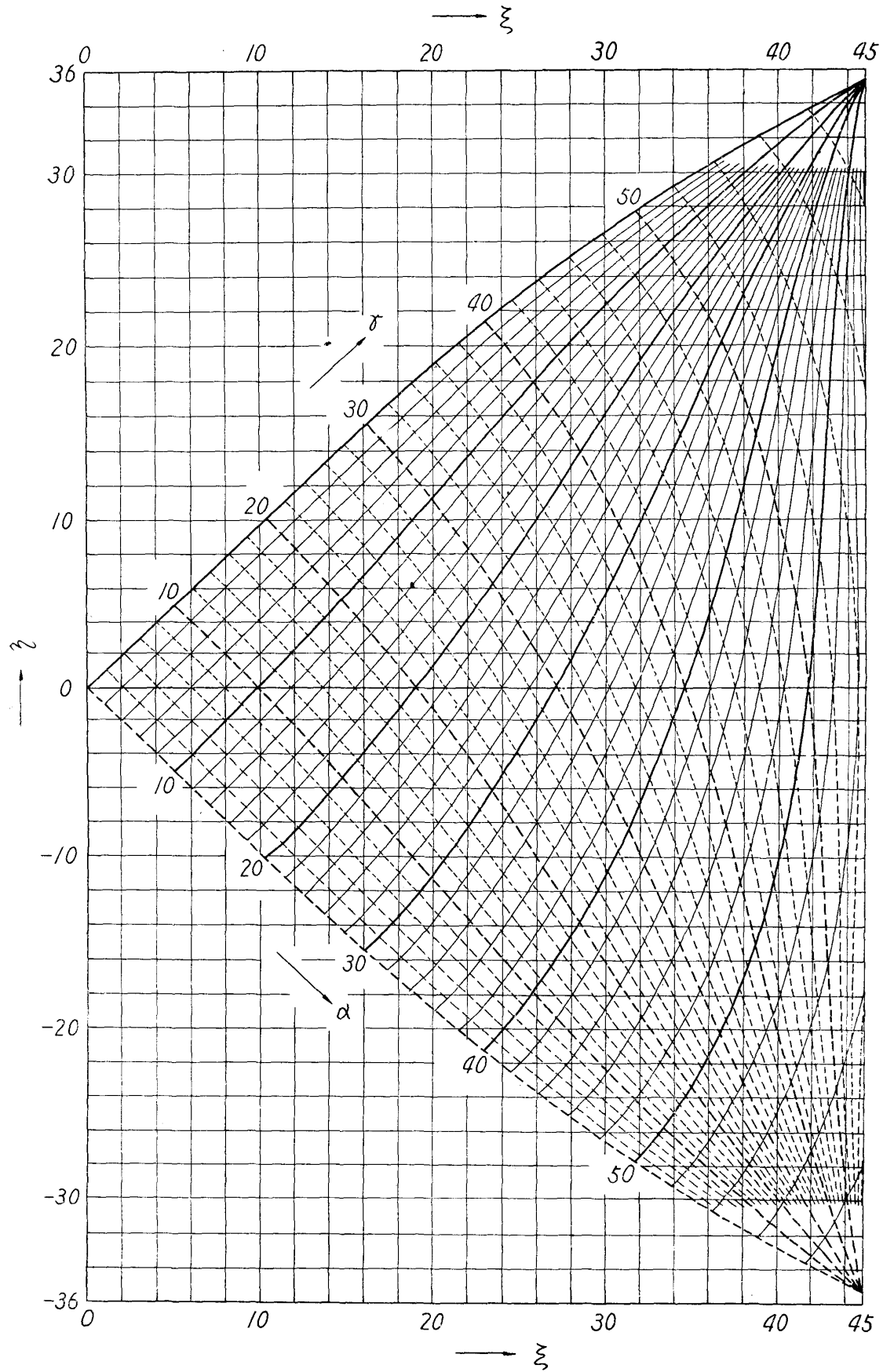


Fig. 2. Isogonic line chart to determine the orientation of surface normal by two angles  $\alpha$  and  $\gamma$  in the case where four  $\{111\}$  traces are in appearance.

with that of  $\gamma$  only at one point. Such a chart is shown in Fig. 2, in which both  $\alpha$  and  $\gamma$  are taken at the interval of two degrees.

In the case where four traces of  $\{111\}$  with different directions are visible on the surface of specimen under a microscope, take the largest angle between two neighbouring traces as angle  $\delta$ , and take the angles  $\alpha$ ,  $\beta$  and  $\gamma$  successively anti-

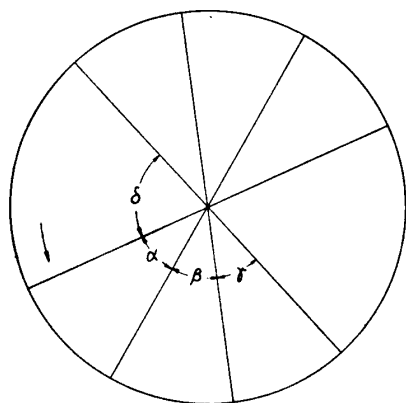


Fig. 3. Definitions of angles  $\alpha$ ,  $\beta$ ,  $\gamma$  and  $\delta$ .

clockwise as shown in Fig. 3. From the angles  $\alpha$  and  $\gamma$ , the orientation of the crystal grain can be determined uniquely and immediately by referring to Fig. 2. When the point indicating the orientation falls on OA or OC,  $\delta = \beta$ ,  $\alpha = 0$  (or  $\gamma = 0$ ); when the point is on ABC,  $\beta = 0$ . In these cases, only three traces will appear on the surface, but as there are other cases in which one of four traces is accidentally lacking, these will be stated in II-3 below. In the special case where the point coincides with  $\langle 111 \rangle$  as stated above, only three traces will appear, but here the unique answer is  $\langle 111 \rangle$ , as the three angles

must be equal to  $60^\circ$ .

## 2. Remarks on using the chart

The accuracy of the orientation determined as above depends solely on whether the markings observed are truly the traces of  $\{111\}$  planes. Further in the present case, there is no room for operational errors to be introduced after the measurement of angles. However, as the changes in  $\alpha$  or  $\gamma$  are not proportional to those in  $\xi$  and  $\eta$  as may be seen from Fig. 2, the angles  $\alpha$  and  $\gamma$  must be measured with sufficiently high accuracy in some ranges of orientation. For example, in the vicinity of  $\{100\}$ , the accuracy with  $1^\circ$  in measuring  $\alpha$  and  $\gamma$  will be rewarded with the same accuracy for both  $\xi$  and  $\eta$ , but in the vicinity of  $\{110\}$ , the same accuracy will entail that of  $\pm 6 \sim 8^\circ$  in determining  $\eta$ , though  $\xi$  may be determined with accuracy of  $1^\circ$ . This possible low accuracy in some cases can not be eliminated, as long as the traces of  $\{111\}$  alone are relied, but little consideration has been paid on this problem in the past.

## 3. The case of three traces of $\{111\}$

Besides the cases with zero value of any one of the angles  $\alpha$ ,  $\beta$  and  $\gamma$  mentioned in II-1, there are cases in which one of the four traces that should naturally appear is absent. For every case of one of the four traces being missing, the chart similar to that shown in Fig. 2 can be made, but upon looking through such charts, it can be deduced that it is impossible to determine the orientation uniquely from the observation of three traces alone. Laying aside the detailed discussion, the possible answers will only be mentioned. Put the largest of the three angles between the three traces  $\alpha'$  and take the angles  $\beta'$  and  $\gamma'$  anti-clockwise. In Fig. 4 are given the number of possible orientations deducible from the measurement

of the angles  $\alpha'$  and  $\gamma'$ . In the figure IBDFHM the possible orientations compatible with any values of  $\alpha'$  and  $\gamma'$  count 2, within AIM: 4, on AJ, AL and IKM: 3, on AI, AK and AM: 3 (of which two are symmetrical), at the points J,

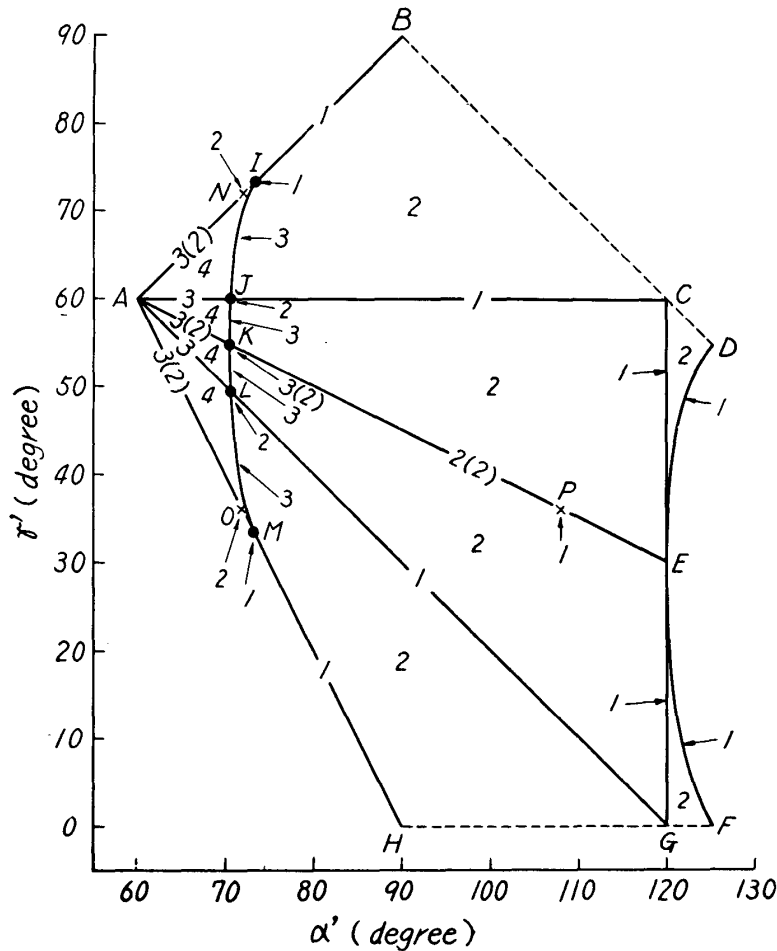


Fig. 4. The relation between the angles ( $\alpha'$ ,  $\gamma'$ ) between three  $\{111\}$  traces and the number of orientations corresponding to these traces.

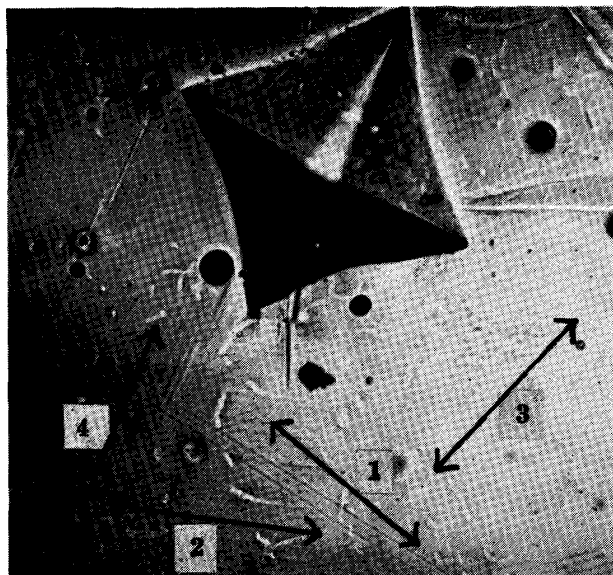
L, N, O: 2, on the line KE: 2 (symmetrical), on the lines IB, JC, LG, MH, CEG and DEF and at the points P, I and M: 1. Thus, only a few sets of three traces are capable of uniquely determining the orientation, usually 2~4 different orientations being deduceable from three  $\{111\}$  traces.

#### 4. Methods of bringing out the $\{111\}$ traces

As mentioned above, annealing twins and slip lines can give rise to  $\{111\}$  traces in face-centred cubic metals. For bringing out the former, the method of thermal etching<sup>(4)</sup> already used by the present authors is very effective, but in general, twins on all the four  $\{111\}$  planes are hardly seen in one crystal grain. In such a case, however, it is possible to bring out traces of all the four  $\{111\}$  planes by producing slip lines with such as a micro-hardness tester. In Photo. 1 is shown the indentation on the surface of a  $\gamma$ -crystal (face-centred cubic) of Fe-30

(4) S. Takeuchi and T. Homma, Sci. Rep. RITU, A9 (1957), 493.

per cent Ni alloy, produced by a micro-hardness tester under 500 g at room temperature. Slip lines in four directions indicated by arrow-marks are seen in the matrix. Of the angles between these lines, that of  $71^\circ$  is the largest, and take



× 350

Photo. 1. Four directions of slip lines produced by pyramid of hardness tester in Fe-30% Ni alloy.

this as  $\delta$ , then  $\alpha=32^\circ$ ,  $\beta=54^\circ$  and  $\gamma=23^\circ$ , from which  $\xi=25.5^\circ$  and  $\eta=-6^\circ$  by referring to Fig. 2.

In most cases, the slip lines brought out by such a method are of two or three different directions. However, when these are utilized together with annealing twins, it is very easy not only to bring out all the  $\{111\}$  traces in one crystal grain, but also to determine the crystal orientation at high temperature by producing indentation in the matrix of mother phase, however small, as in the case of martensite transformation or precipitation at high temperatures. Thus, the method of slip-line is very serviceable for studying the habit plane and the fine structure of transformation products under optical or electron microscope.

### III. The case with $\{100\}$ and $\{111\}$ traces in combination

In the case of  $\{100\}$  traces the table by Tucker and Murphy<sup>(2)</sup> is available, which, however, gives rise to considerable errors, in reading the orientation in some directions; hence, charts were prepared also for the cases where such traces were usable in combination with  $\{111\}$  traces. First, the cases with  $\{100\}$  traces will be stated.

#### 1. The case of $\{100\}$ traces alone

The method for preparing the chart is the same as that in II-1. The orientation of the crystal is shown in Fig. 5, the stereographic projection. The surface of the specimen, the normal of which is shown by the point P within OAB, is

represented by the great circle ①' ②' ③', and when this circle intersects the three {100} planes at the points ①', ②' and ③', these points are the {100} traces on the surface. Denote the angles between ①' and ②', ②' and ③', and ③' and ①' by  $\alpha$ ,  $\beta$  and  $\gamma$ , respectively, then these are correlated with the longitude  $\xi$  and the latitude  $\eta$  in the following way :

$$\cos\alpha = \frac{\cos\xi \tan\eta}{\sqrt{\sin^2\xi + \tan^2\eta}}$$

$$\cos\beta = \frac{\tan\xi \tan\eta}{\sqrt{1 + \sec^2\xi \tan^2\eta}}$$

$$\cos\gamma = \frac{\sin\xi}{\sqrt{\sin^2\xi + \tan^2\eta} \sqrt{1 + \sec^2\xi \tan^2\eta}}$$

Using these formulae, the chart in Fig. 6 may be obtained by the same method as described in the previous chapter.  $\beta$  is the largest concerning any point in the chart (when P is located on OB,  $\alpha = \beta = 90^\circ$ ). The abscissa denotes  $\xi$  and the ordinate  $\eta$ . For the orientation within OBC in Fig. 5, inter-

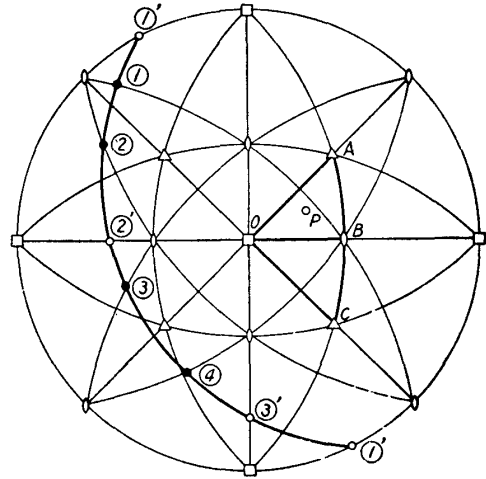


Fig. 5. The stereographic projection showing the poles of the normal of crystal surface, the {100} and the {111} traces.

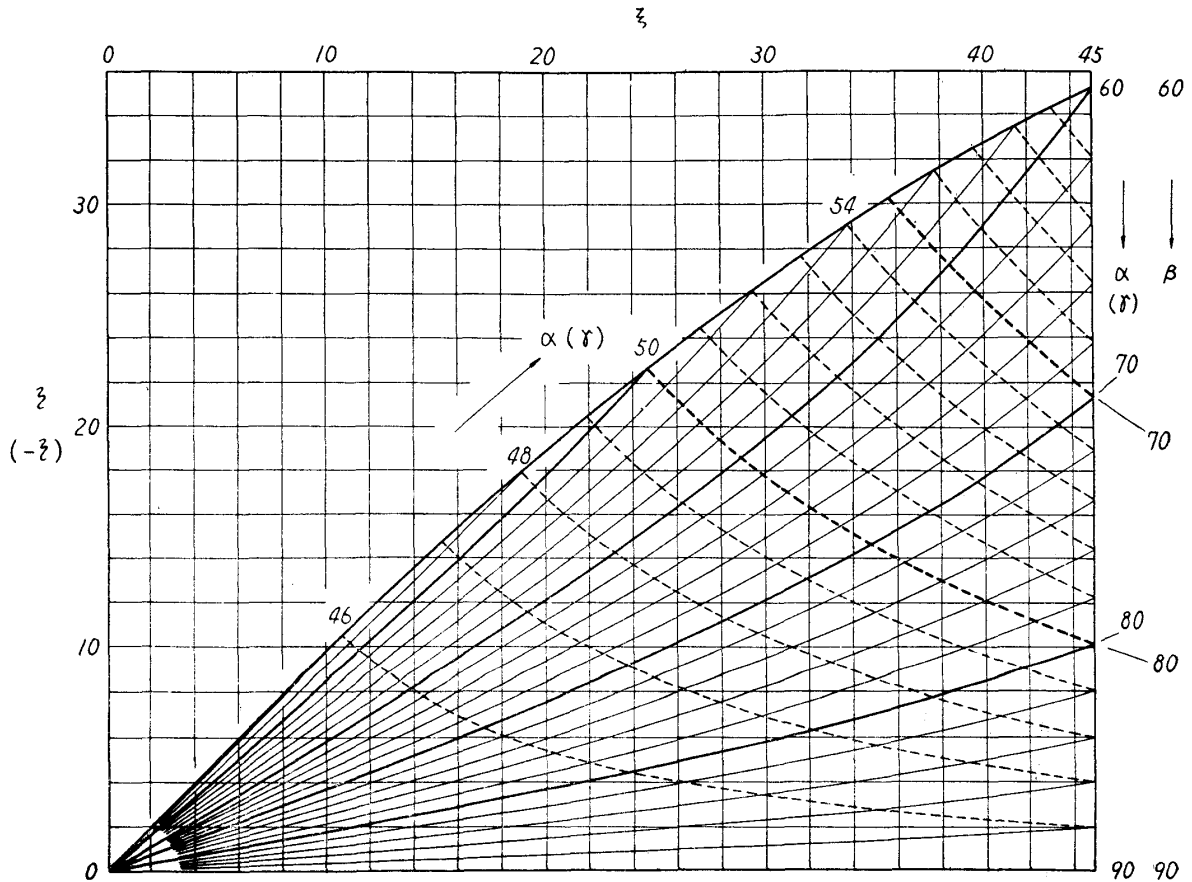


Fig. 6. The chart to determine the orientation of surface normal by using  $\alpha$  or  $\gamma$  and  $\beta$ , in the case where three {100} traces are in appearance.



change  $\alpha$  with  $\gamma$  reversed-image-wise, that is, if  $\gamma$  is substituted for  $\alpha$  in Fig. 6, the chart will indicate the points  $(\xi, -\eta)$ . Therefore, the procedure of determining the orientation by means of the chart shown in Fig. 6 will be as follows: Reproduce the  $\{100\}$  traces as observed on the micro-photograph of the crystal as

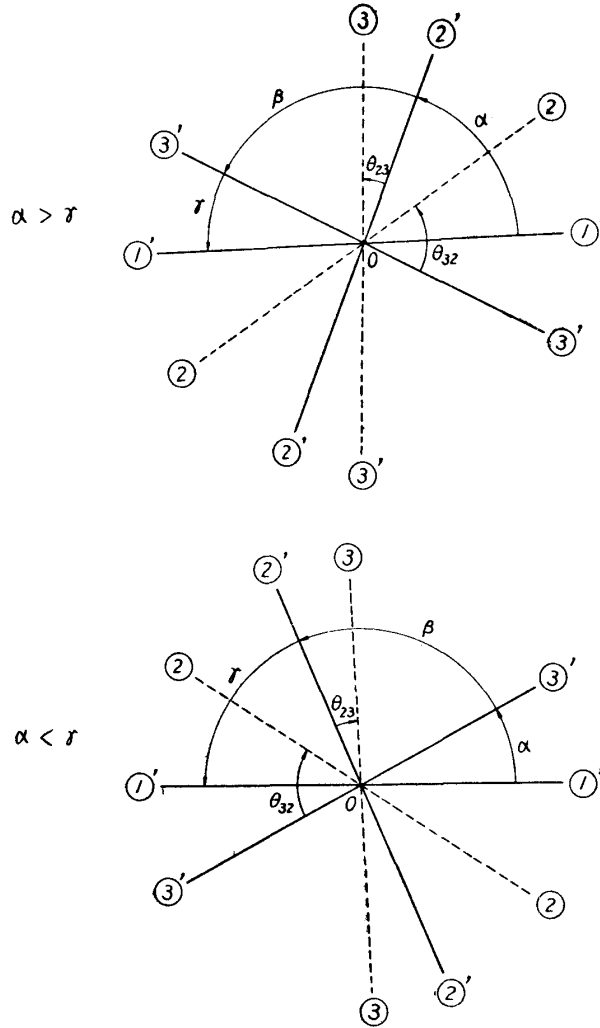


Fig. 7. Definition of angles between  $\{100\}$  and  $\{111\}$  traces.

determination.

## 2 The case of $\{100\}$ traces in combination with $\{111\}$ traces

Only the case will be interpreted in which all the possible  $\{100\}$  traces are fully developed, but with considerable errors unavoidable in the determination of orientation owing to the causes stated in III-1. In these cases, however, it was effective to utilize complementally the traces on  $\{111\}$  planes.

As the traces compatible with the orientation points within the areas OAB and OBC are reflected images of each other, calculations concerning the points within OAB were only made. In the case where the  $\{100\}$  traces come forth as shown in Fig. 7, let  $O2'$  and  $O3'$  stand for the traces forming the largest angle

shown in Fig. 7, denote the largest angle by  $\beta$  and take successively the angles  $\gamma$  and  $\alpha$  always anticlockwise. Using the angles  $\alpha$  and  $\beta$ , or  $\gamma$  and  $\beta$ , the orientation may be determined by reference to Fig. 6. In the cases  $\alpha$  or  $\gamma=0^\circ$ , i. e., when both angles are right (as in the cases of rectangular etch-pits), it is, of course, impossible to determine the orientation by these angles alone. Besides, it is clear that from Fig. 6 that when  $\beta$  is larger than about  $85^\circ$ , the reading may be subject to considerable error, even in the case where three traces are brought out as a triangular etch-pit. So, if the etch-pits brought out form figures approaching a right-angled triangle or a rectangle, it will well-nigh be impossible to determine the orientation with high accuracy, so that some method such as to bring out slip lines, the bottom edges of etch-pits with high precision or twins, if there are producible, have to be taken for the

$\beta$ . The  $\{111\}$  traces usually appear in one or some of the four locations indicated by ①, ②, ③ and ④ in Fig. 5. The angles between ①' on one hand at ①, ②, ③ and ④ on the other are denoted by  $\theta_{11}$ ,  $\theta_{12}$ ,  $\theta_{13}$  and  $\theta_{14}$ , those between ②' on the one hand and ①, ②, ③ and ④ on the other by  $\theta_{21}$ ,  $\theta_{22}$ ,  $\theta_{23}$  and  $\theta_{24}$ , and those between ③' on the one hand and ①, ②, ③ and ④ on the other by  $\theta_{31}$ ,  $\theta_{32}$ ,  $\theta_{33}$  and  $\theta_{34}$ , respectively. All these angles are to be measured anti-clockwise from the lines ①' ②' and ③'. The angle  $\theta_{23}$  is correlated to  $\xi$  and  $\eta$  as follows:

$$\cos\theta_{23} = \frac{(1 + \tan\xi)\tan\eta + (\sin\xi\tan\xi + \cos\xi)}{\sqrt{(\sec\xi\tan\eta + \tan\xi)^2 + (1 + \sec\xi\tan\eta)^2 + (1 - \tan\xi)^2}}$$

Any other angle  $\theta$  can be readily computed from  $\alpha$ ,  $\beta$ ,  $\gamma$ ,  $\theta_{23}$  and the angles between the  $\{111\}$  traces as defined in II-1. The isogonic lines of the twelve angles  $\theta$  are shown in Fig. 3, which shows that for using in combination with

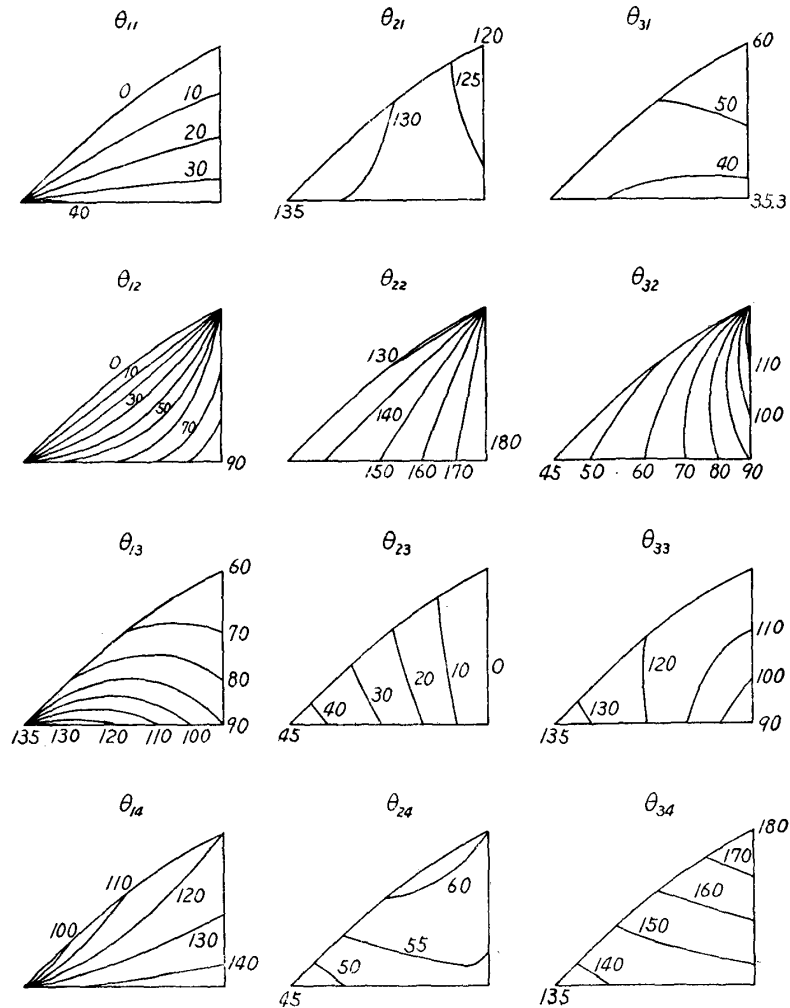


Fig. 8. The isogonic lines of angles between the  $\{100\}$  and the  $\{111\}$  traces.

the isogonic lines of the angle  $\alpha$  or  $\gamma$ , those of  $\theta_{23}$  and  $\theta_{32}$  are most convenient. Of course, the lines for all the angles  $\theta$  are serviceable, but the highest accuracy is obtained when those for  $\theta_{23}$  or  $\theta_{32}$  are used. Individual  $\{111\}$  trace may be

identified by measuring the angles which they form. For example, when ②' is taken as the starting line,  $\theta_{23} < 45^\circ$ ,  $45^\circ < \theta_{24} < ca62^\circ$ ,  $120^\circ < \theta_{21} < 135^\circ$  and  $120^\circ < \theta_{22} < 180^\circ$ . When the range of the possible magnitude of one angle  $\theta$  overlaps with that of the other angle, these should be determined by the angle  $\beta$  as shown below. In the above case, both angles  $\theta_{21}$  and  $\theta_{22}$  may take any value between  $120^\circ$  and  $135^\circ$ , but as the ranges of possible magnitude of  $\beta$  against  $\theta_{21}$  and  $\theta_{22}$  of the same value are different, the discrimination between them is easy. The relations of  $\theta_{22}$  and  $\theta_{21}$  versus  $\beta$  are shown in Fig. 9. Hence, the question whether

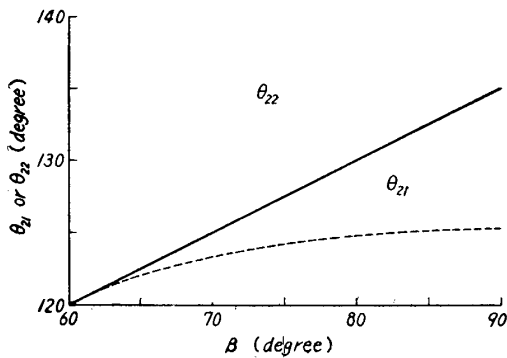


Fig. 9. Relation between  $\theta_{21}$  or  $\theta_{22}$  and  $\beta$ .

a trace appearing at  $130^\circ$  anti-clockwise from ②' represents ① or ② may be answered as follows: If  $\beta > 80^\circ$ , the trace is ①, and if  $\beta < 80^\circ$ , it is ②.

When the orientation is within the area OBC in Fig. 5, the reflected-image relation comes into application, and the angles  $\theta$  must be measured clockwise from ①', ②' and ③' for maintaining the same meaning as mentioned hitherto. Whether the orientation falls within OAB or OBC

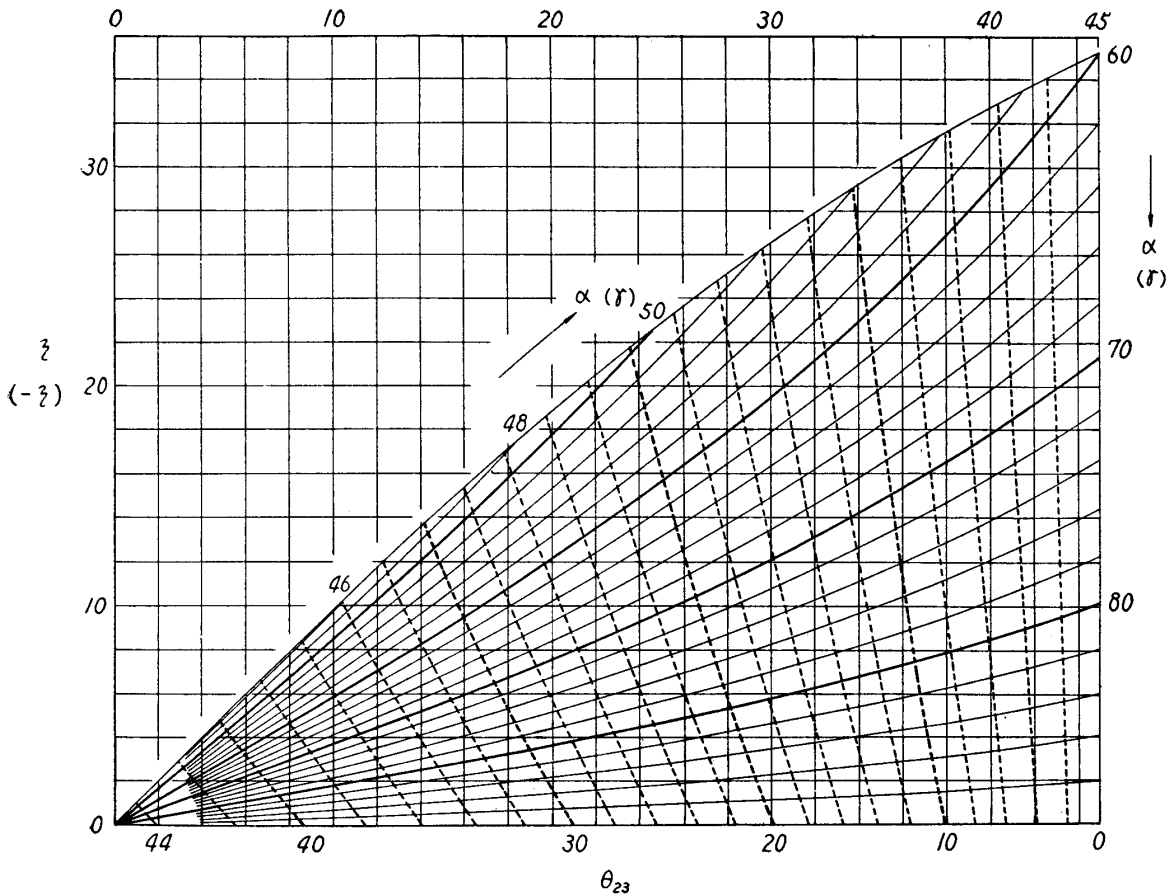


Fig. 10. The chart to determine the orientation of surface normal by using  $\alpha$  or  $\gamma$  and  $\theta_{23}$ .

is determined by the relative values of  $\alpha$  and  $\gamma$  as described in III-1 above, that is, when  $\alpha > \gamma$ ,  $\eta$  is positive, and when  $\alpha < \gamma$ ,  $\eta$  is negative.

Fig. 10 shows the chart of  $\alpha$  and  $\theta_{23}$  in the case of both positive  $\xi$  and  $\eta$ , or that of  $\gamma$  and  $\theta_{23}$  in the case of positive  $\xi$  and negative  $\eta$ . Fig. 11 shows the

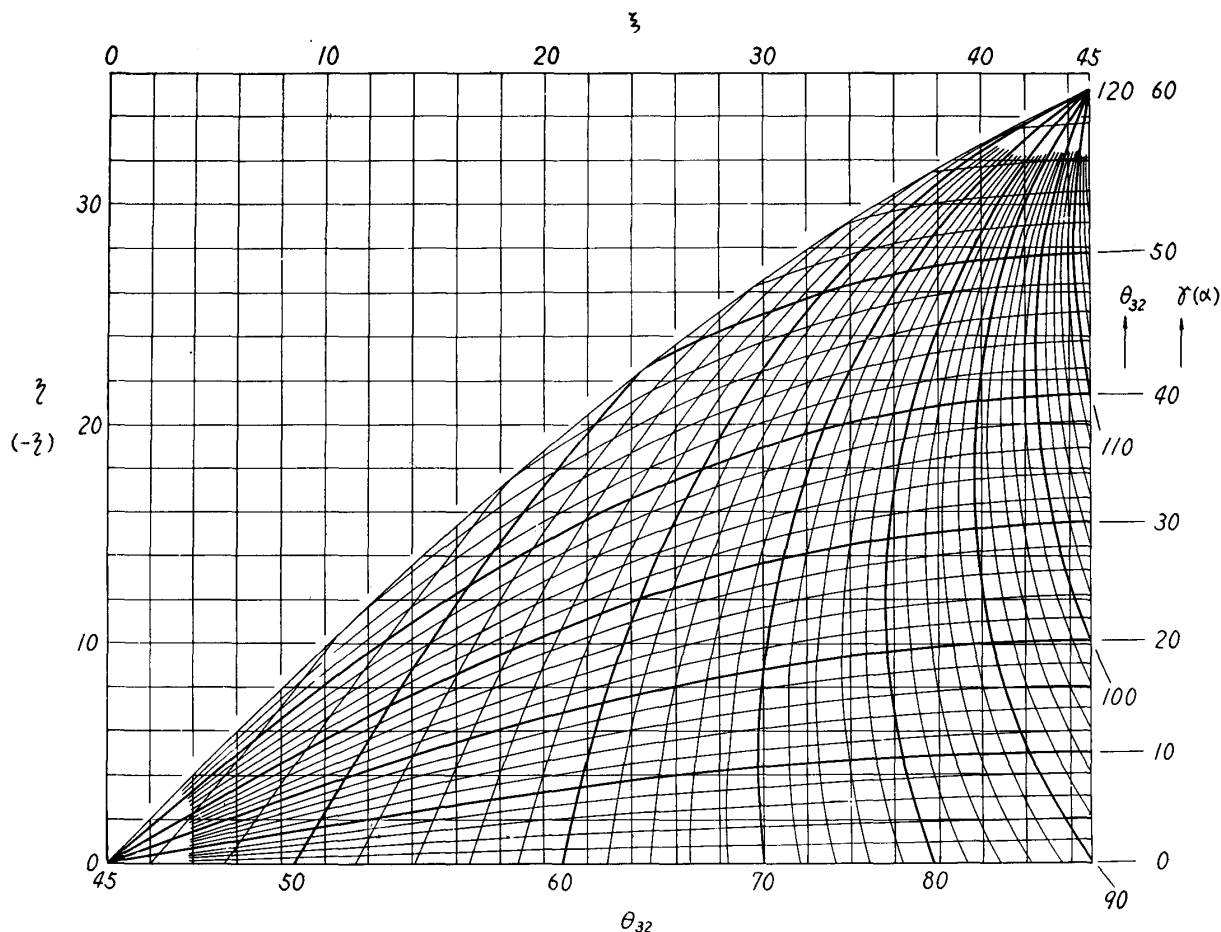


Fig. 11. The chart to determine the orientation of surface normal by using  $\alpha$  or  $\gamma$  and  $\theta_{32}$ .

chart of  $\gamma$  and  $\theta_{32}$  ( $\xi, \eta$ ), or that of  $\alpha$  and  $\theta_{32}$  ( $\xi, -\eta$ ).

To determine the orientation by means of these charts, the angles between the  $\{100\}$  traces must first be measured, and when  $\alpha > \gamma$ , that is,  $\eta$  is positive, a  $\{111\}$  trace must be found in the range between  $0^\circ$  and  $45^\circ$  measured anti-clockwise from the line  $O(2)'$ , or in the range between  $45^\circ$  and  $120^\circ$  anti-clockwise from  $O(3)'$  in Fig. 7; when  $\alpha < \gamma$ , a similar traces must be found in the range  $0 \sim 45^\circ$  clockwise from  $O(2)'$ , or  $45^\circ \sim 120^\circ$  clockwise from  $O(3)'$ .

If a twin is seen at such angles, these can be readily utilized, but in other cases, slip lines of two or three directions can be readily formed by pressing the grain with the a micro-Vickers hardness tester, and the best adapted of these lines may serve for the purpose.

Photo. 2 is a photograph showing etch-pits and slip lines on a specimen of pure (99.99 per cent) aluminium. The specimen was first electrolytically polished

with perchloric acid anhydride, then etched with 50 per cent aquatic solution of aqua regia to produce pits and pricked with a needle to make slip lines. In this case, the sides of the etch-pits were  $\{100\}$  traces and the slip lines were  $\{111\}$

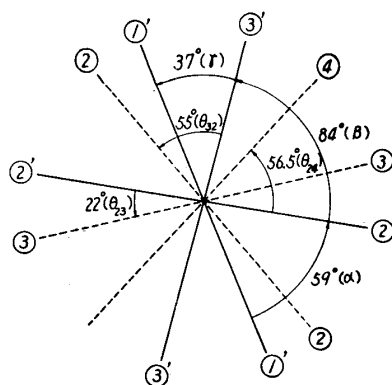
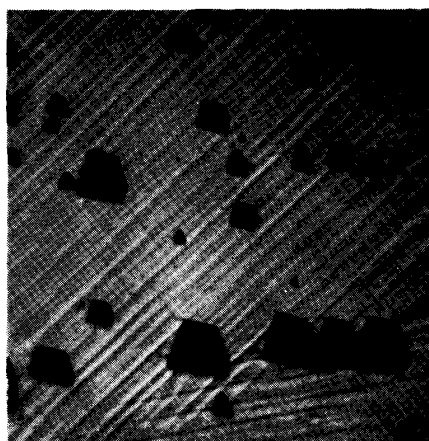


Fig. 12. Angles between  $\{100\}$  and  $\{111\}$  traces in Photo. 2.



×150

Photo. 2. Etch pits and slip lines in pure Al.

traces. As shown in Fig. 12, of the angles between the three  $\{100\}$  traces, take the largest (the angle of  $84^\circ$ ) as  $\beta$ , then  $\alpha=59^\circ$  and  $\gamma=37^\circ$ , so that  $\alpha>\gamma$ ; in this case, therefore, measure the angles between  $\textcircled{2}'$  and the  $\{111\}$  traces anti-clockwise, then  $\theta_{23}=22^\circ$  and so forth. With these values of  $\alpha$  and  $\theta_{23}$ , the orientation of  $\xi=23^\circ$  and  $\eta=15^\circ$  can readily be obtained from Fig. 10. From Fig. 6 it follows that  $\xi=22.5^\circ$  and  $\eta=14.5^\circ$ , and in the case of this order of  $\beta$ , the orientation can approximately be determined without reference to the slip lines. In most cases, however, it is rather difficult to determine the exact directions of the sides of the etch-pits, and it would be less likely to cause errors, when Figs. 6, 10 and 11 are used in appropriate combination, utilizing not only the  $\{100\}$  traces but also slip lines etc. as well.

### Summary

(1) For the purpose of simplifying the procedure of determining the orientation of

individual crystallite in an aggregate, examinations were made of twins, slip-lines, etch-pits and such surface traces, and charts showing the relations of the angles between such traces and the crystal orientation were prepared.

(2) The relation between the number of different orientations compatible with the same angles between the traces was made clear in the cases where only three  $\{111\}$  traces were in appearance, and the intertrace angles which were capable of determining the orientation in such cases were schematically showed.

(3) It was shown that even in the case of a triangular etch-pits — a case in which the orientation was presumed to be determinable unequivocally — if one of the angles is larger than about  $85^\circ$ , the danger of introducing a considerable error is not excluded. In consideration of this danger, charts were drawn by using the  $\{111\}$  traces in combination with the  $\{100\}$  traces, and it was made clear that only two of the four  $\{111\}$  traces were usable in such combinations for the accurate determination of the orientation of crystal-grains.

### **Acknowledgments**

The present authors must state with appreciations that this study was made possible by the allocation of a part of the Scientific Research Fund by the Education Ministry.